

## Effect of Copper Additions on The Properties of Recycled Pure Aluminum Chips

*Noha Naeim*

*Department of Production Engineering and Mechanical Design, Port Said University, Port Fouad 42526, Egypt.*

*Email :noha.fouaad@eng.psu.edu.eg, DOI: 10.21608/PSERJ.2023.204326.1228*

### ABSTRACT

The effect of copper addition for recycled pure aluminum chips on microstructure, mechanical properties, and wear behavior has been investigated. The wear behavior was carried out at various applied loads, wearing times, and revolution of specimens, with the process responses being the obtainable microstructure, tension test, hardness, and wear loss. The results showed that increasing the copper content by up to 6 wt.% increased the number of grain boundaries and their constituents. Furthermore, large agglomerates have formed in some areas, most notably in the 10 wt.% Cu sample. In addition, 8 wt.% Cu sample exhibits optimal behavior, as its uniform dispersion aids in enhancing the mechanical and tribological characteristics of Al-Cu alloys. The minimum and maximum ultimate tensile stress values were obtained with recycled pure aluminum chips and an 8 wt.% Cu addition. The minimum wear value was 0.012 gm at a spindle speed of 90 rpm at copper percentage of 10 wt.%. The maximum wear value was 70.8 gm at a spindle speed of 350 rpm at a copper percentage of 0 wt.%.

**Keywords:** Hardness, Cu Additions, Wear Losses, Mechanical Properties, Microstructure, And Aluminum Recycling.

*Received 5-4-2023*

*Revised 13-4-2023*

*Accepted 19-4-2023*

© 2023 by Author(s) and PSERJ.

*This is an open access article licensed under the terms of the Creative Commons Attribution International License (CC BY 4.0).*

<http://creativecommons.org/licenses/by/4.0/>



## 1. INTRODUCTION

Aluminum is a material that infinitely recyclable; approximately 75% of all aluminum produced in history is still in use today [1]– [3]. On average, one-third of the aluminum used today is made from recycled scrap [2]. Recycling entails by re-melting, which uses only 5% of the energy required to produce new aluminum from bauxite ore [4]. When it comes to sustainability, aluminum has two facets [5], [6]. Firstly, reduces energy consumption in products and processes such as lightweight transportation, packaging, and construction due to its low mass density in addition to its high electrical and thermal conductivities and appropriate corrosion behavior [7], [8]. Secondly, aluminum is one of the most significant emitters of greenhouse gases (GHG) and one of the most energy-intensive industrial metals derived from ores [4], [9].

Aluminum is also one of the most malleable metals on the planet. Application of aluminum in industry including a wide range of items such as cans, cooking utensils, aerospace, aircraft components, and marine

industries, have been produced due to their high strength-to-weight ratio [10]. On the other hand, pure aluminum metal is much too soft for such applications, and it lacks the high tensile strength required for aircraft and helicopters, so various alloying elements are added to aluminum to improve its mechanical properties [11].

Grain refining is the modification of the solidification process to induce more grains to form and the grains to form in a specific shape [12]. Severe plastic deformation (SPD), as one of the successful top-down techniques in the last thirty years, has the ability to refine materials in the order of ultrafine grains or nanostructures [13]–[15]. The term "refining" is mostly used to refer to adding chemical additives to metal, although it may also refer to controlling the cooling rate. The material which added to a liquid metal to produce finer grain size in the subsequent casting is referred to as a grain refiner [16].

Copper is the most often used parent metal and alloying element in the manufacture of alloy materials for a wide range of technical applications. In addition to, copper and its alloys are well-known for their moderate hardness, ductility, toughness, high electrical

conductivity, machinability, and corrosion resistance [17]. Their usage of overhead wire has decreased because of its high surface area to volume ratio. They are nevertheless employed as an alloy for architectural applications, biofuel resistance, electrical house wiring, and others. Copper's toxicity to aquatic bacteria and algae has contributed to its usage in alloy creation for underwater applications [18].

A variety of methods, including cold working, heat treatment, and the addition of alloying elements to the aluminum matrix, can be used to enhance aluminum characteristics. The addition of alloying components such as minor elements, major elements, and microstructure impurities can be used to manage the alloy's required strength. From the last two decades, due to the increase in demand from the electricity transmission lines, copper is being replaced by Al because of its light weight and relatively low cost [19], [20]. Copper additions also increase the hardness and strength of aluminum casting alloys at all temperature levels and heat treatment conditions, resulting in improved machinability of the produced alloys [21], [22].

Lee et al. [23] investigated the dimensional stability and microstructure of two Zn–Al ternary alloys in both as-cast and heat-treated circumstances. The results showed that Zn–Al alloys were better than SAE phosphor bronze in terms of wear resistance and dimensional stability.

L. Jian et al. [24] investigated the wear characteristics of the ZA-27 alloy by substituting silicon for copper and modifying the microstructure of Si with strontium. The results showed that the modified alloy has the best wear resistance.

B.K. Prasad et al. [25] examined the dry sliding wear behavior of zinc-aluminum alloys and compared it to conventional zinc-aluminum alloys and leaded tin bronze. The authors found that leaded tin bronze has a lower wear resistance than standard zinc-aluminum alloys.

The current paper aimed to carry out a systematic study to investigate the effect of adding 2, 4, 6, 8, and 10 wt.% high purity copper to recycled pure aluminum chip on its metallurgical microstructure, tension, hardness, and wear resistance in the cast condition.

## 2. EXPERIMENTAL WORK

In the current study, recycled pure aluminum chip (98.49 wt.% Al) were used in addition with copper as a major alloying element. The chemical composition of aluminum was analyzed using SPECTROLAB device and listed in **Table 1**

**Table1: Chemical composition of pure aluminum chip and Al-Cu alloys**

element	Cu	Si	Zn	Fe	Mg	Mn	V	Ti	Al
Base	0.45	0.234	0.0205	0.729	0.0401	0.0233	0.00414	0.00896	Bal
I (2wt.% Cu)	2.44	0.178	0.0472	0.277	0.0373	0.0143	0.0173	0.0289	Bal
II (4wt.% Cu)	4.85	0.194	0.0386	0.182	0.0315	0.0148	0.0176	0.0215	Bal
III (6wt.% Cu)	6.36	0.198	0.0482	0.375	0.0311	0.0128	0.0151	0.0198	Bal
IV (8wt.% Cu)	8.18	0.219	0.0457	0.492	0.0466	0.0179	0.0173	0.0215	Bal
V (10wt.% Cu)	10.93	0.126	0.001	0.108	0.056	0.0212	0.00435	0.00345	Bal

Recycled pure aluminum chip were melted in the graphite crucible and casted in copper tube with a 300-mm-long, 30-mm-diameter. However, copper was added to a crucible as a powder wrapped in foil and then mixed for five minutes by flipping it. In this experiment, a resistance furnace was used. According to the Al-Cu phase diagram as shown in **Fig. 1**[26], the pouring temperature for all castings was 750 °C. Copper was added to the melt in various weights as refinement additions: 2, 4, 6, 8, and 10 wt.%. Furthermore, all specimens were subjected to a casting heat treatment (annealing) in order to relieve the stresses that obtain within a casting during solidification.

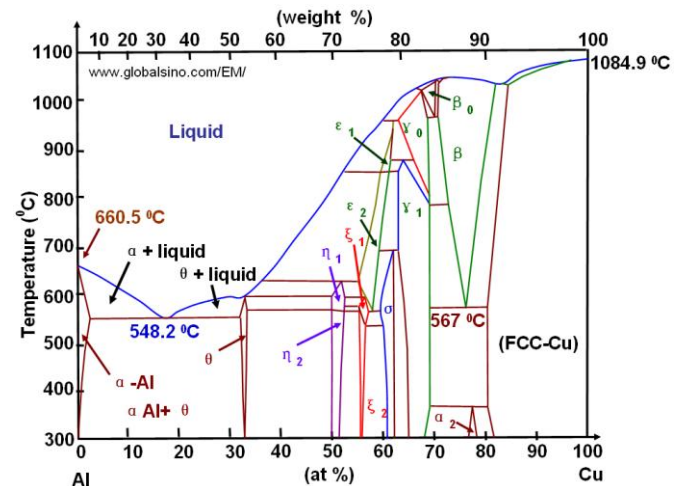


**Figure 1: Phase diagram of Al-Cu binary alloy[26].**

In the muffle furnace, heat was applied to 15 samples (three samples for each addition), then, they were kept at 300°C for two hours before cooling to room temperature (22°C). After annealing, the cast specimens were divided into five samples (tension, hardness, microstructure, and wear) and then machined to the specified dimensions for the test specimen according to the standard. The

microstructure specimens were prepared for the removal of fine scratches by grinding with SiC abrasive papers and polishing with Al<sub>2</sub>O<sub>3</sub> suspension solutions of various abrasive sizes. A light microscope was used to examine the microstructure properties of each of the experimental alloys. Furthermore, tension test results with specimen dimensions according to ASTM standards shown in **Fig. 2** were used to assess the mechanical behavior of each recycled pure aluminum chip and Al-Cu alloy specimen.

Three specimens with the same chemical composition were examined for each testing condition, and the average value of their results was obtained to establish the reliability of the mechanical test results. The tension test was carried out using a universal testing machine. For hardness, specimens of 29 mm in diameter and 15 mm in height were prepared. The Brinell hardness (HB) of each recycled pure aluminum chip and Al-Cu alloy specimen was measured using a hardness tester (Qness 3000) and a 5 mm Brinell tungsten ball with an applied load of 30Kgf. The average Brinell hardness (BH) was determined by taking three measurements on the surface of each specimen. Dry sliding wear tests were carried out using a pin-on-disc device (as shown in **Fig. 3**) by using a cylindrical specimen with 20 mm in diameter and 50 mm in height against a steel disc of 85 mm in diameter. The wear test was carried out under different conditions of wear time, applied pressure, and rotational speed. Wear time values were taken as 15, 30, 45, and 60 min; applied pressure values were 0.195, 0.351, 0.507, and 0.664 MPa; and rotational speed values were 90, 224, and 350 rpm.

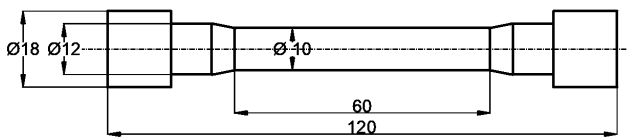


**Figure 2: Dimensions for the tensile specimen (mm).**

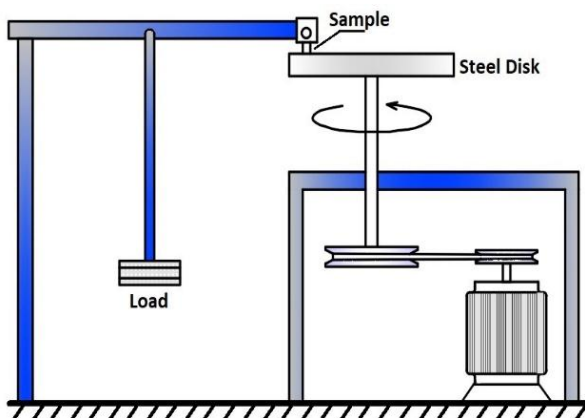


**Figure 3: Pin-on-disc device.**

### 3. RESULTS AND DISCUSSION

#### 3.1 Effect Of Copper Addition on Metallurgical Structure

Figure 3 depicts light micrographs of Al-Cu casting alloys with different Cu additions. The pristine aluminum matrix has a regular grain form and size, and few pores are seen, as shown in **Figure 4a**. With Cu concentration rising, an increase in the number of grain boundaries and their constituents is noticed in the microstructure, indicating a grain refining feature. This phenomenon was observed in samples containing up to 6% Cu (**Figs. 4b, c, and d**). A uniform fine Al<sub>2</sub>Cu matrix is obviously composed primarily of fine Al<sub>2</sub>Cu dispersion at grain boundaries. Interestingly, when the wt.% of Cu increases, the volume fraction of the precipitated phase near grain boundaries in the aluminum matrix increases significantly. The ability to achieve such a uniform stable dispersoids fine grain distribution using traditional technology and recycled material provides a significant advantage to metal composites intended for use in high-strength applications.

Notably, this is only possible with an alloy dispersoid configuration in which the interfacial energies, solid-state diffusivity, and elemental solubility are minimized, hence limiting coarsening and interfacial reactions. Furthermore, the arrangement and size of  $\alpha$ -Al phase and eutectic Cu particles are influenced by differences in local solidification time between the wall and centre portions of a cast component, for instance, from the wall (high solidification rate) to the core (lower solidification rate). In high solidification, the  $\alpha$ -Al morphology mostly displayed a globular shape in regions adjacent to wall sections. This subsequently evolved into dendrites and branches that moved towards the center (as shown in **Fig.5**). Thus, there is a large driving force for precipitation, and nucleation starts quickly, homogeneously, and in many places. In case of tiny amount Cu, according to Al-Cu phase diagram, Al- $\alpha$  phase contains large, dissolved Cu than required for equilibrium. As a result, produce a proper Al<sub>2</sub>Cu precipitate is difficult in that case [27].

However, as the Cu additive concentration increases, agglomeration and an unequal distribution of additives in the matrix are depicted in **Figures 4(e, f)**. The distribution of Cu is not uniform, and bigger agglomerates have developed in certain areas, particularly for 10 wt.% Cu. Cu agglomerates and forms new, huge grains surrounded by an intermetallic phase at the interfaces. This might be explained by the impact of substantial density variations on the dispersion of copper blends.



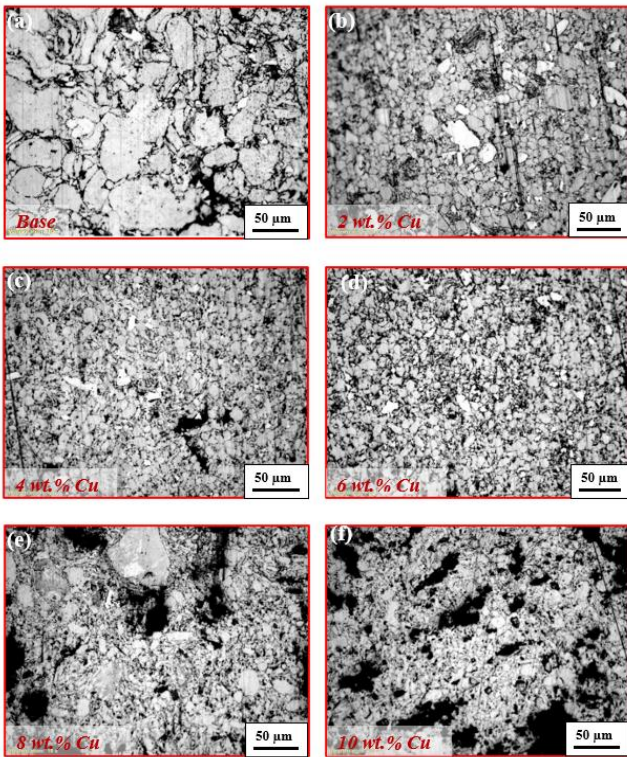


Figure 4: Light micrographs (LM) of casting samples with different copper additions.

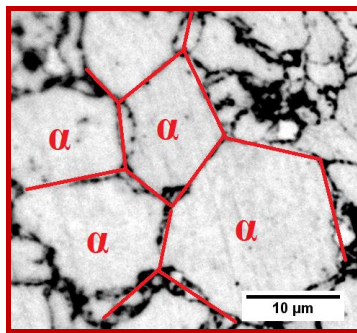


Figure 5: High magnification micrographs of Al-4 wt.% Cu with emphasized Al- $\alpha$  phase and grain boundaries (red lines)

### 3.2 Effect of Copper Addition on Stress Strain Curve

The effect of copper addition to recycled pure aluminum chip at various weights (2, 4, 6, 8, and 10 wt.%) on the stress-strain curve is shown in **Figure 6**.

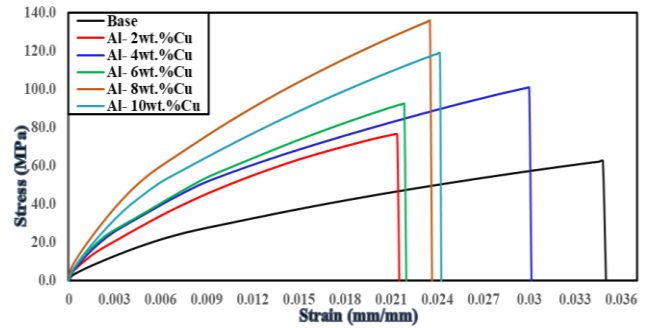


Figure 6: Stress- Strain curve for pure Al compared with constant additives percentage of Cu.

**Figure 6** represents the relationship between stress and strain for recycled pure aluminum chip and with different copper additions. Ultimate stress increased until an 8 wt.% copper addition, then decreased with a 10 wt.% copper addition. The minimum ultimate tensile stress was 60.56 MPa at recycled pure aluminum chip, and the maximum ultimate tensile stress was 133.77 MPa at 8 wt.% Cu addition which was 120% higher than the pristine sample. It is important to note that the ultimate stresses for the first three additions were comparable, and that the 4 wt.% sample exhibited apparent ductility. This result similar to previous studies[22]. The microstructure indicates that the exceptional performance is primarily due to the fine homogeneous grain distribution; however, the poor elongation is due to the presence of a significant amount of pore and void defects. As a consequence, the precipitation process that occurs as a result of  $Al_2Cu$  may be associated with increases in dislocation density, which restricts dislocation slip mobility and improves mechanical properties[28]. Continuous Cu addition reduces the precipitation of intermetallics, which is correlated with strength improvements [29]. The use of AlCu alloying resulted in a significant increase in yield stress, which may be an incentive to minimize any mechanical characteristics sacrificed.

### 3.3 Effect of Copper Additions on Hardness

**Figure 7** depicts the change in hardness as a function of copper percentage in recycled pure aluminum chip and test alloys. Al-2 wt.% Cu alloy hardness increased to 25.5 BHN, enhanced by 40% compared to the as-cast sample, this trend was permanent up to 8 wt.% concentrated alloy with a hardness of 67, with enhancement by 168 %, represent the peak value. With high concentrations of Cu content (10 wt.%) retaining its typical dendrite structure with marginal decline in hardness of 67 BHN, which still higher than pristine sample. The hardness of the aluminum alloy with Cu increased as the fraction of Cu particulates by weight increased up and then decreased afterward[30][31].

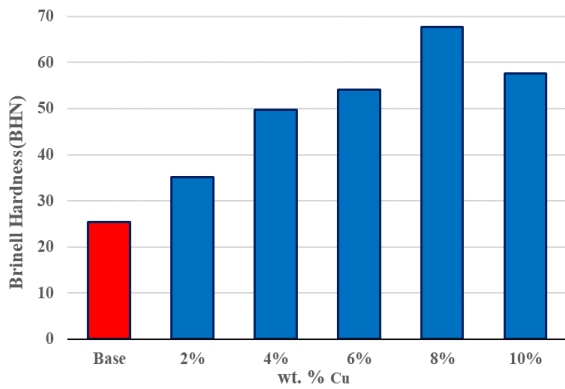


Figure 7: Effect of copper content on the Brinell hardness test.

### 3.4 Effect of Copper Addition on Wear Behavior

An investigation was carried out on recycled pure aluminum chip at various copper percentage weights at four different loads and times (5, 10, 15, and 20 kg) and (15, 30, 45, and 60 min), respectively. The resultant wear losses for recycled pure aluminum chip obtained at the considered spindle speed ranges of 90, 224, and 350 rpm are presented in Figs. 8, 9, and 10, respectively.

As shown in **Figs. 8, 9, and 10**, the lowest weight loss was recorded at higher copper percentages. The minimum wear value was 0.012 gm at a spindle speed of 90 rpm, a load of 5 kg, a time of 15 minutes, and a copper percentage of 10 wt.%. The maximum wear value was 70.8 gm at a spindle speed of 350 rpm, a load of 20 kg, a time of 60 minutes, and a copper percentage of 0 wt.% (pristine sample). The decrease in wear losses can be attributed to the increasing copper percentage, which increases the thermal conductivity and, therefore, reduces the surface temperature [32].

and time increase. The minimum value of wear occurred at a load of 5 kg and a time of 15 min with 10 wt.% Cu.

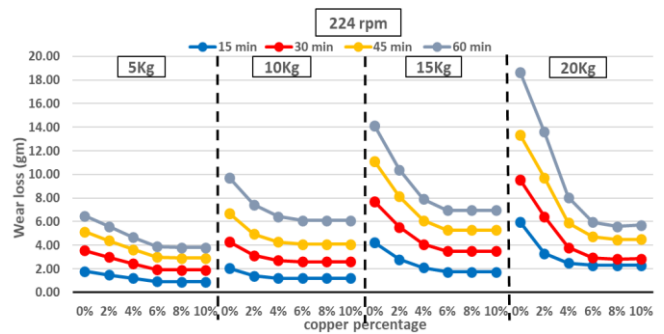


Figure 9: Effect of copper addition on the wear loss with different loads and times at spindle speed of 224 rpm.

**Figure 9** shows the relationship between wear loss and copper percentage for various loads, times, a 224 rpm. It is noticeable that all of the figures show the same tendency. The results show that the wear loss increases as the applied load and time increase. The lowest value of wear occurred at a weight of 5 kg and a period of 15 min, whereas the highest value of wear occurred at a load of 20 kg and a time of 60 min.

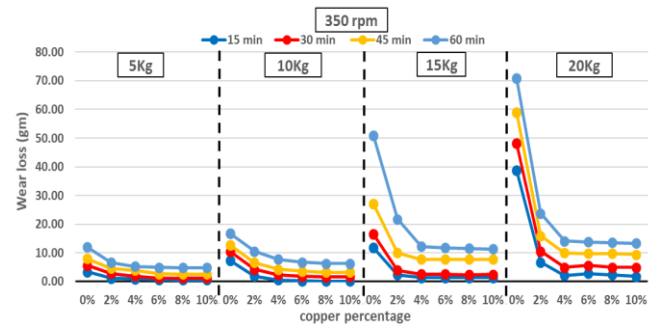


Figure 10: Effect of copper addition on the wear loss with different loads and times at spindle speed of 350 rpm.

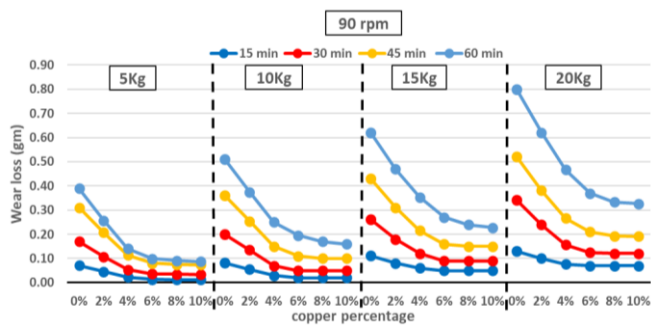


Figure 8: Effect of copper addition on the wear loss with different loads and times at spindle speed of 90 rpm.

The effects of varied loads and times on wear losses at a spindle speed of 90 rpm are shown in **Figure 8**. It can be shown that changes in loads have an effect on the wear results. This can be seen since all wear results follow the same trend. Wear loss increases as both load

**Figure 10** shows the effect of varied applied load and time on wear loss at a spindle speed of 350 rpm. It is seen that all of the figures show the same tendency. The results reveal that the wear loss increases as the applied load and time increase. The minimum value of wear occurred at a load of 5 kg and a time of 15 minutes, while the maximum value of wear occurred at a load of 20 kg and a time of 60 min.

It can be seen from the graphs that the cumulative weight loss of the alloyed samples will increase as the sliding-distances during tests increase. The results were essentially the same throughout the entire tests. The results showed that the participated phase projected into the samples remained attached to the work surface throughout the entire test. Notably, at highest load and speed, instead of cracking, the soft aluminium particles erode easily, leading to surface roughness of the sliding-samples. This discovery was made after continuous

contact with the disc surface revealed the disturbed grain structures inside the sample.

Because the roughness of the mixed elements was not projected and the entire surface was exposed to equal tension, the roughness may readily deform, resulting in a higher initial wear rate as the ripped and undamaged sample surface ploughed both the pin and disc (see Figs. 8, 9). Many shattered aluminium particles aggressively projected onto the disc, where they would eventually form debris and plough in the sample, leading to a greater initial wear rate. Contact between the two surfaces, aided by the pin to expand the contact area, resulted in nearly constant strain on the aluminium surface, which in turn led to increased stress and wear [32]. Wear-rate falls progressively in but remains almost constant in the case of highly loaded Cu samples as the sliding-distance (represent rpm) grows with constant load. In accordance with the findings of numerous studies, the results show that as the load rises, so does the frictional force, leading to a greater degree of disengagement and eventual sample failure [33], [34]. Said simply, After the material's surface tension is broken, the abrasive wear effect is over, stabilising the forces at play and allowing the first stage of adhesive processes to manifest [35]. Moreover, when the sliding revolution rises, the material's initial hardness may change, mostly due to a surface softening effect on the material, which is promoted by the rise in temperature in the contact region.

## 4. CONCLUSIONS

A systematic study of the evolution of the microstructural features, mechanical properties, and wear resistance of recycled pure aluminum chip with varying Cu contents was conducted, and the following conclusions were reached:

- Increasing the copper content up to 6% increases the number of grain boundaries and their constituents, which is noticed in the microstructure, indicating a grain refining feature.
- The Cu distribution is not uniform, and larger agglomerates have formed in some areas, particularly in the 10 wt.% Cu sample.
- The 8 wt.% Cu sample exhibits optimal behavior, as its uniform dispersion aids in enhancing the mechanical and tribological characteristics of composites.
- Tensile stress increased until an 8 wt.% copper addition, then decreased with a 10 wt.% copper addition. The minimum ultimate tensile stress was 60.56 MPa at recycled pure aluminum chip, and the maximum ultimate tensile stress was 133.77 MPa at 8 wt.% Cu addition.

- The minimum wear value was 0.012 gm at a spindle speed of 90 rpm, a load of 5 kg, a time of 15 minutes, and a copper percentage of 10%. The maximum wear value was 70.8 gm at a spindle speed of 350 rpm, a load of 20 kg, a time of 60 minutes, and a copper percentage of 0%.

**Acknowledgments:** This work was supported by the Production Engineering and Mechanical Design department's lab at Faculty of Engineering, Port Said University.

## 5. REFERENCES

- [1] D. Raabe *et al.*, "Making sustainable aluminum by recycling scrap: The science of 'dirty' alloys," *Prog. Mater. Sci.*, vol. 128, no. March, 2022. <https://doi.org/10.1016/j.pmatsci.2022.100947>.
- [2] T. Graedel, J. Allwood, and M. Buchert, "DigitalCommons @ University of Nebraska - Lincoln What Do We Know About Metal Recycling Rates?," 2011.
- [3] T. E. Graedel, E. M. Harper, N. T. Nassar, and B. K. Reck, "On the materials basis of modern society," *Proc. Natl. Acad. Sci. U. S. A.*, vol. 112, no. 20, pp. 6295–6300, 2015. <https://doi.org/10.1073/pnas.1312752110>.
- [4] T. G. Gutowski, S. Sahni, J. M. Allwood, M. F. Ashby, and E. Worrell, "The energy required to produce materials: Constraints on energy-intensity improvements, parameters of demand," *Philos. Trans. R. Soc. A Math. Phys. Eng. Sci.*, vol. 371, no. 1986, 2013. <https://doi.org/10.1098/rsta.2012.0003>.
- [5] D. Raabe, C. C. Tasan, and E. A. Olivetti, "Strategies for improving the sustainability of structural metals," *Nature*, vol. 575, no. 7781, pp. 64–74, 2019. <https://doi.org/10.1038/s41586-019-1702-5>.
- [6] J. L. Cann *et al.*, "Sustainability through alloy design: Challenges and opportunities," *Prog. Mater. Sci.*, vol. 117, 2021. <https://doi.org/10.1016/j.pmatsci.2020.100722>.
- [7] P. Mukhopadhyay, "Alloy Designation, Processing, and Use of AA6XXX Series Aluminium Alloys," *ISRN Metall.*, vol. 2012, no. Table 1, pp. 1–15, 2012. <https://doi.org/10.5402/2012/165082>.
- [8] R. jie FAN, S. ATTARILAR, M. SHAMSBORHAN, M. EBRAHIMI, C. GÖDE, and H. V. ÖZKAVAK, "Enhancing mechanical properties

- and corrosion performance of AA6063 aluminum alloys through constrained groove pressing technique,” *Trans. Nonferrous Met. Soc. China (English Ed.)*, vol. 30, no. 7, pp. 1790–1802, 2020.  
[https://doi: 10.1016/S1003-6326\(20\)65339-0](https://doi.org/10.1016/S1003-6326(20)65339-0).
- [9] J. M. Allwood, J. M. Cullen, and R. L. Milford, “Options for achieving a 50% cut in industrial carbon emissions by 2050,” *Environ. Sci. Technol.*, vol. 44, no. 6, pp. 1888–1894, 2010.  
[https://doi: 10.1021/es902909k](https://doi.org/10.1021/es902909k).
- [10] B. Vijaya Ramnath, C. Parswajinan, R. Dharmaseelan, K. Thileepan, and K. Nithin Krishna, “A review on aluminium metal matrix composites,” *Mater. Today Proc.*, vol. 46, pp. 4341–4343, 2021.  
[https://doi: 10.1016/j.matpr.2021.03.600](https://doi.org/10.1016/j.matpr.2021.03.600).
- [11] N. Nafsin and H. M. M. A. Rashed, “Effects of copper and magnesium on phase formation modeling and mechanical behavior in Al-Cu-Mg alloys,” *Int. J. Automot. Mech. Eng.*, vol. 8, no. 1, pp. 1151–1161, 2013.  
[https://doi: 10.15282/ijame.8.2013.6.0094](https://doi.org/10.15282/ijame.8.2013.6.0094).
- [12] R. Ibrahim, E. Soeudy, G. A. El-Nasser, A. El-Megharbel, A. El-Baghdady, and R. I. El-Soeudy, “Influence of Grain Refining on The Mechanical Properties and Tribological Behavior for Pure Aluminum,” *Proc. ninth Cairo Univ. Int. Conf. Mech. Des. Prod.*, no. October, pp. 895–906, 2008.
- [13] R. Z. Valiev and T. G. Langdon, “Principles of equal-channel angular pressing as a processing tool for grain refinement,” *Prog. Mater. Sci.*, vol. 51, no. 7, pp. 881–981, 2006.  
[https://doi: 10.1016/j.pmatsci.2006.02.003](https://doi.org/10.1016/j.pmatsci.2006.02.003).
- [14] A. P. Zhilyaev and T. G. Langdon, “Using high-pressure torsion for metal processing: Fundamentals and applications,” *Prog. Mater. Sci.*, vol. 53, no. 6, pp. 893–979, 2008.  
[https://doi: 10.1016/j.pmatsci.2008.03.002](https://doi.org/10.1016/j.pmatsci.2008.03.002).
- [15] F. Djavanroodi, M. Ebrahimi, and J. F. Nayfeh, “Tribological and mechanical investigation of multi-directional forged nickel,” *Sci. Rep.*, vol. 9, no. 1, pp. 1–9, 2019.  
[https://doi: 10.1038/s41598-018-36584-w](https://doi.org/10.1038/s41598-018-36584-w).
- [16] A. Nassef, “Modification of AA7075 Alloy by Addition of Al-5Ti-1B Alloy Modification of AA7075 Alloy by Addition of Al-5Ti-1B Alloy,” no. June, 2016.  
[https://doi: 10.13140/RG.2.1.2601.6246](https://doi.org/10.13140/RG.2.1.2601.6246).
- [17] J. O. Agunsoye, S. A. Bello, S. B. Hassan, R. G. Adeyemo, and J. M. Odii, “The Effect of Copper Addition on the Mechanical and Wear Properties of Grey Cast Iron,” *J. Miner. Mater. Charact. Eng.*, vol. 02, no. 05, pp. 470–483, 2014.  
[https://doi: 10.4236/jmmce.2014.25048](https://doi.org/10.4236/jmmce.2014.25048).
- [18] K. B. Lee, Y. S. U. Kim, and H. Kwon, “Fabrication of Al-3 Wt Pet Mg Matrix Composites Reinforced with Al<sub>2</sub>O<sub>3</sub> and SiC Participates by the Pressureless Infiltration Technique,” *Metall. Mater. Trans. A Phys. Metall. Mater. Sci.*, vol. 29, no. 12, pp. 3087–3095, 1998.  
[https://doi: 10.1007/s11661-998-0216-9](https://doi.org/10.1007/s11661-998-0216-9).
- [19] H. S. Abdo, K. A. Khalil, M. M. El-Rayes, W. W. Marzouk, A. F. M. Hashem, and G. T. Abdel-Jaber, “Ceramic nanofibers versus carbon nanofibers as a reinforcement for magnesium metal matrix to improve the mechanical properties,” *J. King Saud Univ. - Eng. Sci.*, vol. 32, no. 5, pp. 346–350, 2020.  
[https://doi: 10.1016/j.jksues.2019.03.008](https://doi.org/10.1016/j.jksues.2019.03.008).
- [20] H. S. Abdo, A. H. Seikh, J. A. Mohammed, and M. S. Soliman, “Alloying elements effects on electrical conductivity and mechanical properties of newly fabricated al based alloys produced by conventional casting process,” *Materials (Basel)*, vol. 14, no. 14, 2021.  
[https://doi: 10.3390/ma14143971](https://doi.org/10.3390/ma14143971).
- [21] Y. Chen *et al.*, “Influences of Cu content on the microstructure and strengthening mechanisms of Al-Mg-Si-xCu alloys,” *Metals (Basel)*, vol. 9, no. 5, 2019.  
[https://doi: 10.3390/met9050524](https://doi.org/10.3390/met9050524).
- [22] R. A. Gonçalves and M. B. Da Silva, “Influence of Copper Content on 6351 Aluminum Alloy Machinability,” *Procedia Manuf.*, vol. 1, pp. 683–695, 2015.  
[https://doi: 10.1016/j.promfg.2015.09.014](https://doi.org/10.1016/j.promfg.2015.09.014).
- [23] M. M. Khan and M. Nisar, “Effect of in situ TiC reinforcement and applied load on the high-stress abrasive wear behaviour of zinc–aluminum alloy,” *Wear*, vol. 488–489, no. January 2021, p. 204082, 2022.  
[https://doi: 10.1016/j.wear.2021.204082](https://doi.org/10.1016/j.wear.2021.204082).
- [24] L. Jian, E. E. Laufer, and J. Masounave, “Wear in Zn-Al-Si alloys,” *Wear*, vol. 165, no. 1, pp. 51–56, May 1993.  
[https://doi: 10.1016/0043-1648\(93\)90371-R](https://doi.org/10.1016/0043-1648(93)90371-R).
- [25] B. K. Prasad, A. K. Patwardhan, and A. H. Yegneswaran, “Dry sliding wear characteristics of



some zinc-aluminium alloys: a comparative study with a conventional bearing bronze at a slow speed,” *Wear*, vol. 199, no. 1, pp. 142–151, Nov. 1996.  
[https://doi: 10.1016/0043-1648\(96\)07231-6](https://doi.org/10.1016/0043-1648(96)07231-6).

[26] X. Liu *et al.*, “Solidification of Al-xCu alloy under high pressures,” *J. Mater. Res. Technol.*, vol. 9, no. 3, pp. 2983–2991, 2020.  
[https://doi: 10.1016/j.jmrt.2020.01.049](https://doi.org/10.1016/j.jmrt.2020.01.049).

[27] C. D. S. Tuck, C. A. Powell, and J. Nuttall, “Corrosion of Copper and Its Alloys,” in *Reference Module in Materials Science and Materials Engineering*, Elsevier, 2016.

[28] A. M. Al-Obaisi, E. A. El-Danaf, A. E. Ragab, M. S. Soliman, and A. N. Alhazaa, “Statistical Model for the Mechanical Properties of Al-Cu-Mg-Ag Alloys at High Temperatures,” *Adv. Mater. Sci. Eng.*, vol. 2017, pp. 1–13, 2017.  
[https://doi: 10.1155/2017/1691465](https://doi.org/10.1155/2017/1691465).

[29] Z. Cheng *et al.*, “Effect of Cu and Mg addition on the mechanical and degradation properties of Zn alloy wires,” *J. Biomater. Appl.*, vol. 37, no. 5, pp. 891–902, 2022.  
[https://doi: 10.1177/08853282221123934](https://doi.org/10.1177/08853282221123934).

[30] T. Balarami Reddy, P. Karthik, and M. Gopi Krishna, “Mechanical behavior of Al–Cu binary alloy system/ Cu particulates reinforced metal-metal composites,” *Results Eng.*, vol. 4, no. October, p. 100046, 2019.  
[https://doi: 10.1016/j.rineng.2019.100046](https://doi.org/10.1016/j.rineng.2019.100046).

[31] A. Wakif, Z. Boulahia, S. R. Mishra, M. Mehdi Rashidi, and R. Sehaqui, “Influence of a uniform transverse magnetic field on the thermo-hydrodynamic stability in water-based nanofluids with metallic nanoparticles using the generalized Buongiorno’s mathematical model,” *Eur. Phys. J. Plus*, vol. 133, no. 5, 2018.  
[https://doi: 10.1140/epjp/i2018-12037-7](https://doi.org/10.1140/epjp/i2018-12037-7).

[32] H. Sharudin *et al.*, “Effect of copper on friction and wear properties of copper-based friction materials,” *J. Tribol.*, vol. 21, no. September 2018, pp. 13–20, 2019.

[33] G. E. Kiourtsidis and S. M. Skolianos, “Wear behavior of artificially aged AA2024/40  $\mu\text{m}$  SiCp composites in comparison with conventionally wear resistant ferrous materials,” *Wear*, vol. 253, no. 9–10, pp. 946–956, Nov. 2002.  
[https://doi: 10.1016/S0043-1648\(02\)00216-8](https://doi.org/10.1016/S0043-1648(02)00216-8).

[34] S. O’Dell, J. Charles, M. Vlot, and V. Randle, “Modelling of iron dissolution during hot dip galvanising of strip steel,” *Mater. Sci. Technol.*, vol. 20, no. 2, pp. 251–256, Feb. 2004.  
[https://doi: 10.1179/026708304225011289](https://doi.org/10.1179/026708304225011289).

[35] S. C. Lim, M. Gupta, L. Ren, and J. K. M. Kwok, “The tribological properties of Al–Cu/SiCp metal–matrix composites fabricated using the rheocasting technique,” *J. Mater. Process. Technol.*, vol. 89–90, pp. 591–596, May 1999.  
[https://doi: 10.1016/S0924-0136\(99\)00067-9](https://doi.org/10.1016/S0924-0136(99)00067-9).